

Diode-pumped 1988-nm Tm:YAP laser mode-locked by intracavity second-harmonic generation in periodically poled LiNbO₃

H. Cheng, X. D. Jiang, X. P. Hu,* M. L. Zhong, X. J. Lv, and S. N. Zhu

National Laboratory of Solid State Microstructures and School of Physics, Nanjing University, Nanjing 210093, China

*Corresponding author: xphu@nju.edu.cn

Received December 18, 2013; revised March 6, 2014; accepted March 7, 2014;

posted March 7, 2014 (Doc. ID 203192); published March 31, 2014

We report a diode-pumped intracavity second-harmonic generation mode-locked solid-state Tm:YAP laser operating at 1988 nm using a periodically poled congruent LiNbO₃ as the nonlinear crystal. The threshold of continuous wave mode locking is 11.6 W. The maximum output power is 1.67 W, while the shortest pulse obtained is 4.7 ps at a repetition rate of 97.09 MHz. © 2014 Optical Society of America

OCIS codes: (140.4050) Mode-locked lasers; (140.3070) Infrared and far-infrared lasers; (140.5680) Rare earth and transition metal solid-state lasers; (160.4330) Nonlinear optical materials.

<http://dx.doi.org/10.1364/OL.39.002187>

Solid-state ultrafast mode-locked lasers in the 2- μm wavelength region have received increasing interests in recent years due to their broad applications in photomedicine, remote sensing, optical communication, time-resolved molecular spectroscopy, minimally invasive surgery, as well as pumping sources for coherent x-ray generation and synchronously pumped optical parametric oscillators operating in the mid-infrared region around and above 5 μm [1–6]. In the past two decades, Tm³⁺-doped, and Tm³⁺, Ho³⁺-codoped materials have been used as laser gain media to realize ultrafast 2- μm lasers through both active [7–9] and passive mode-locking approaches. Compared with an active mode-locking scheme, passively mode-locked 2- μm lasers not only have the advantages of reliability, simplicity and compactness, but also can generate much shorter pulses. In most passively mode-locked 2- μm lasers, ultrafast pulses are produced by using intracavity saturable absorbers (SAs). By using a semiconductor saturable absorber mirror (SESAM), pulses at around 2 μm with durations ranging from several tens of picoseconds [10] to a few picoseconds [11,12], even down to hundreds of femtoseconds [13,14], have been achieved. Besides, PbS quantum-dot-doped glass SAs are also promising candidates for 2- μm Q-switched mode locking [15,16]. Recently, single-walled carbon nanotubes [17–19], graphene oxide absorbers [20], and graphene SAs [21] showed great potential for 2- μm mode locking. The reported pulses durations range from a few picoseconds to hundreds of femtoseconds with different laser gain crystals.

Other than SA methods, intracavity frequency doubling is a promising passively mode-locking approach and there are mainly two mechanisms. The first one is a frequency-doubling nonlinear mirror (FDNLM) [22]. A FDNLM can provide a low self-starting threshold but has the disadvantage of longer pulse duration due to group velocity mismatch (GVM). The second mechanism is cascaded second-order nonlinear mode locking (CSM), which has a relatively high self-starting threshold, but it contributes substantially to pulse shortening, and can help to achieve continuous-wave mode locking (CWML) [23–26]. In both schemes, the frequency-doubling crystal

can be either birefringence-phase-matching materials or quasi-phase-matching (QPM) ones. When QPM materials are used as intracavity frequency-doubling crystals, it is feasible to realize mode locking at any wavelength in the nonlinear crystal's transparent spectral range, especially for those lasers working at wavelengths where no SESAMs exist. Up to now, intracavity frequency-doubled mode locking using QPM materials has been reported at 1.064 μm [27] and 1.3 μm [28,29]; however, as far as we know, there are no reports on the realization of mode locking at around 2 μm using this scheme. In this Letter, we demonstrated, for the first time to our knowledge, a diode-pumped Tm:YAP ultrafast laser operating at 1988 nm based on the CSM scheme. The nonlinear crystal used was a periodically poled LiNbO₃ (PPLN) and the average output power reached watt level.

The schematic experimental layout of the mode-locking laser at 2- μm spectral region is shown in Fig. 1. The laser gain media is an a-cut 3 at. % Tm:YAP crystal with the dimensions of 8 mm \times 4 mm \times 4 mm, and it is coated for antireflection ($R < 1\%$) at 795 and 1988 nm on the two 4 mm \times 4 mm end faces. The laser crystal was mounted in a circulating-water-cooled copper holder and was end pumped through M1 by a 30-W fiber-coupled laser diode at 795 nm. The output beam from the fiber was imaged by an optical coupling system onto the laser crystal, generating a 200- μm beam diameter inside the laser gain crystal. M1 is a flat mirror placed very close to the Tm:YAP crystal and is coated for antireflection ($T > 98\%$) at

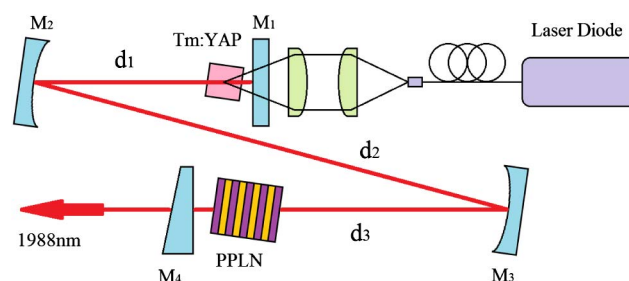


Fig. 1. Scheme of intracavity SHG mode-locked 1988-nm laser with PPLN.

795 nm on both surfaces and high reflection ($R > 99\%$) coated at 1988 nm on the left side. M2 and M3 are two concave mirrors coated for high reflection ($R > 99\%$) at 1988 nm on their concave sides with radius of curvature being 500 and 200 mm, respectively. They were arranged with an incident angle below 5° to minimize astigmatism. M4, the output coupler, is a 5° -wedged dichroic mirror with high reflection ($R > 99.5\%$) at 994 nm and partial transmittance ($T = 3\%$) at 1988 nm on the right side.

The $15\text{ mm} \times 3\text{ mm} \times 0.5\text{ mm}$ PPLN has a poling period of $28.75\text{ }\mu\text{m}$, fabricated using the conventional electrical-field poling technique at room temperature [30]. The two end faces of PPLN are antireflection ($T > 99\%$) coated at both 1988 and 994 nm. The PPLN crystal was put into a home-made oven with precise temperature control ($\pm 0.1^\circ\text{C}$) and was placed very close to the output coupler M4. Both the PPLN and the laser crystal were tilted to avoid Fabry–Perot effect, which may interrupt mode locking. The distances d_1 , d_2 , d_3 (as indicated in Fig. 1) were designed to be 440, 950 and 132 mm, respectively, providing a mode size of $350\text{ }\mu\text{m}$ at the Tm:YAP crystal as well as an $148\text{-}\mu\text{m}$ one at PPLN. Considering the pump spot diameter, which is $200\text{ }\mu\text{m}$, this set of cavity parameters can provide a soft aperture in the laser gain media.

In the experiment, the PPLN crystal was tilted by 11.46° , which corresponded to an actual period of $28.88\text{ }\mu\text{m}$, and this period can be used for frequency doubling of 1988 nm at 150°C . We measured the dependences of the output power on the incident pump power in both CW and ML cases, as shown in Fig. 2. At first, we set the temperature of PPLN to 100°C , which was far from the phase-matching temperature point, and studied the continuous-wave (CW) operation of the laser system. The system started to lase at 2.1-W pumping power, and a maximum output power of 2.74 W was obtained at a pumping power of 25.3 W, with the slope efficiency being $\sim 12.9\%$. Then the crystal temperature was set to 162°C , and the temperature-induced phase mismatch was calculated to be $+5.3\text{ rad}$ at this temperature using the Sellmeier equation of LN [31]. The $+5.3\text{ rad}$ phase mismatch corresponds to a negative nonlinear phase shifting, which represents a diverging cascaded $\chi^{(2)}$ lens. By careful alignment, oscillation started with a threshold of 3.9 W, but mode locking could not be activated at this pumping power level, the laser system was still working in CW mode. When the pumping power reached 7.7 W, Q-switched mode-locking (QML) pulses were observed with an output power of 380 mW. When the pumping power was further raised up to 11.6 W, stable 720-mW CWML was obtained. The output power increased with the pumping power, and the maximum average output power was 1.67 W under a pumping power of 22.6 W with a slope efficiency of 8.2%. As the pump power exceeded 23.5 W, the CWML output became unstable and the output power began to fall because of the thermal lens effect in the laser gain media.

The CWML waveform was detected with a high-speed InGaAs detector (ET-5000) and a digital oscilloscope (Tektronix DPO 7254). The oscilloscope traces are shown in Fig. 3. Here we used the DPX (Tektronix' digital phosphor technology) mode to better reflect the stability

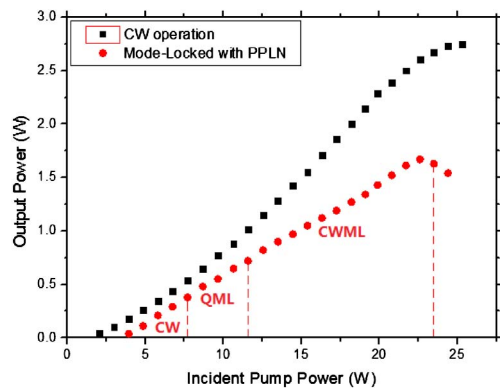


Fig. 2. Output power versus incident pump power in CW and ML regimes.

of the pulse train. As shown in Fig. 3(a), the mode-locked pulse train is clear and sharp, and the DC component is effectively reduced. The time interval between neighboring pulses is 10.3 ns, and this corresponds to a 97.09-MHz repetition rate, which agrees well with the 1522-mm long laser cavity. The CW characteristic of the mode-locked pulse train is evident in Fig. 3(b). The pulse-to-pulse amplitude fluctuation is estimated to be less than 5% in millisecond scale. The CWML output can be sustained for several hours with a power fluctuation less than 3%. Besides, the CWML operation can be repeated every time without any re-adjustment of the optical elements.

Figure 4 shows the spectral properties in both CW and CWML operations. They were measured with an optical spectrum analyzer (YOKOGAWA AQ6375) with a resolution of 0.05 nm. The spectrum of the free-running CW Tm:YAP laser in Fig. 4(a) has several separated emitting lines at around 1988 nm, which was ensured by the coating properties of the mirrors as well as the cavity configuration used in the experiment. The maximum intensity was not located at 1988 nm, and this mainly attributed to the longitudinal mode competition in the free-running laser. The spectrum of the CWML laser has a Gaussian pulse shape with the peak at 1988 nm and a FWHM of 1.06 nm.

Theoretically, all longitudinal modes within the bandwidth of the laser gain crystal should be stimulated and oscillate in a mode-locked form. The fluorescence

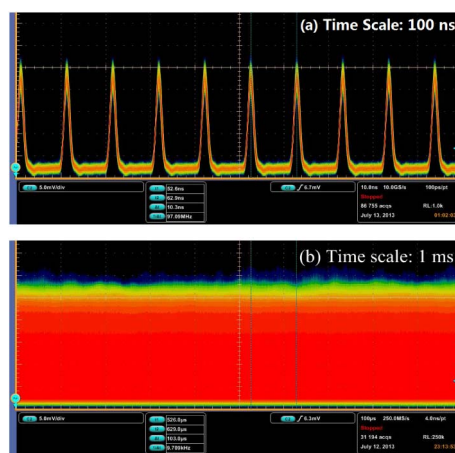


Fig. 3. Oscilloscope traces of pulse train in different time scales: (a) 100 ns and (b) 1 ms.

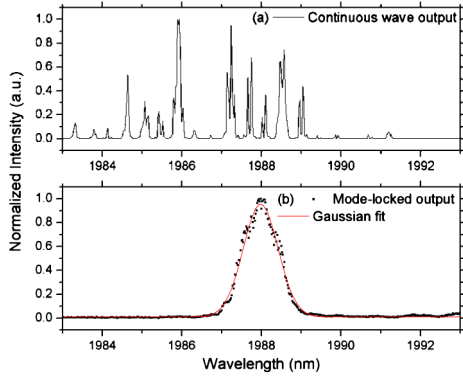


Fig. 4. Output spectra in (a) CW and (b) CWML regimes.

bandwidth of Tm:YAP is about 200 nm and it can support femtosecond mode-locked output according to the Fourier transform limit of the time-bandwidth product supposing no limiting factors. We calculate the dependences of the nonlinear phase shift and the double-pass second-harmonic generation (SHG) efficiency in the 15-mm-long PPLN on the phase mismatch, as shown in Fig. 5. The phase mismatch in the experiment is +5.3 rad, which lies in the envelope of the second peak of the SHG tuning curve. From Fig. 5 we can see that the +5.3 rad phase mismatch corresponds to a proper nonlinear phase shift as well as a proper SHG efficiency. The “allowed” bandwidth acceptance within the envelope of the second peak is about 1.5 nm, which agrees well with the 1.06 nm pulse width obtained in the experiment.

The autocorrelation traces of CWML 1988-nm pulses were measured with an autocorrelator (FR-103XL), and the autocorrelator utilized a background-free (non-collinear) SHG for the measurement of ultrashort laser pulses. As shown in Fig. 6, the pulse duration is 4.7 ps at an output power of 1.05 W, while it is 6.5 ps at 1.67 W maximum output. The time-bandwidth products in both cases are 0.378 and 0.523, corresponding to 1.20 times and 1.66 times that of the Fourier transform limit with a sech^2 pulse shape, respectively. The asymmetrical shapes may result from the asymmetrical beam shapes of the incident beams as well as the GVM-induced pulse distortions. The pulse time-bandwidth product under the maximum average output power is larger than that under the lower power. This phenomenon is due to the inverse loss saturation of CSM [23], and a detailed analysis is as follows.

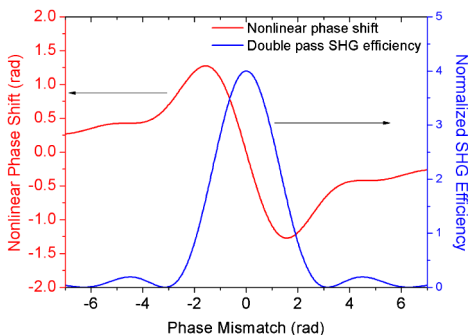


Fig. 5. Normalized double-pass SHG efficiency and nonlinear phase shift versus phase mismatch.

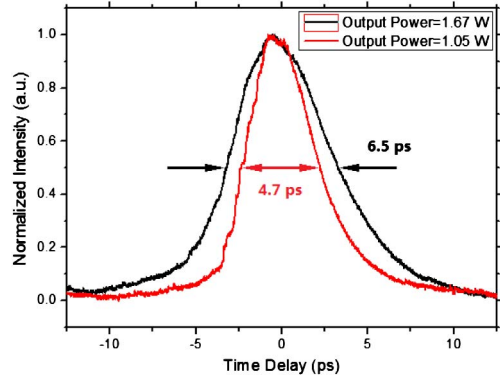


Fig. 6. Autocorrelation traces of mode-locked 1988-nm laser pulses at average output powers of 1.67 and 1.05 W, respectively.

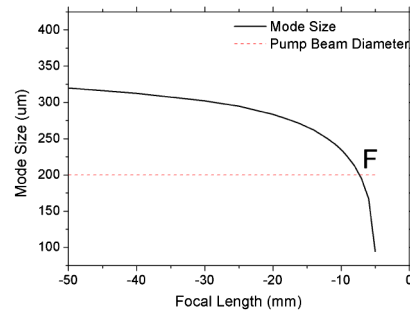


Fig. 7. Mode size in Tm:YAP crystal versus focal length of the cascaded $\chi^{(2)}$ lens.

Figure 7 shows how the mode size inside the Tm:YAP crystal varies with the focal length of the diverging cascaded $\chi^{(2)}$ lens. A critical point, where the mode size in the Tm:YAP crystal is equal to the 200- μm pump spot, is indicated as “F” in Fig. 7. The mode size decreases with the focal length of the diverging cascaded $\chi^{(2)}$ lens, and on the left side of the critical point “F,” higher instantaneous intensity will lead to better overlapping between mode size and pump spot in the gain media and this positive feedback can help with the ML formation. When the pulse instantaneous intensity exceeds the critical point “F,” negative feedback occurs and it can inhibit QML but may broaden the pulse width at the same time.

It should be mentioned that the double pass through the 15-mm-long PPLN would cause a 4.4 ps GVM between the fundamental wave and the second-harmonic wave, which is comparable with the pulse duration obtained in the experiment. The 4.4-ps GVM would surely broaden the pulse duration to some extent. However, in the CSM scheme, GVM can produce a positive cascaded Kerr lens in the initial part of the pulse while it increases the negative Kerr lens in the trailing edge, thus will serve as an efficient pulse shortening mechanism [26]. Besides, the group velocity dispersion in the PPLN crystal, as well as in the laser gain crystal, was calculated to be less than 1 fs for a round trip in the laser cavity, which has little influence on pulse broadening. From the above analysis, we can see that GVM and the length of the nonlinear crystal are the two main limiting factors in the CSM

approach. To further shorten the output pulses even down to femtoseconds, some optimum compensations should be implemented, and short PPLN crystals are preferred though requesting higher intracavity peak powers.

In summary, we have successfully constructed a picosecond solid-state laser in the 2- μm spectral region based on the CSM scheme. Near-transform-limit pulses with 6.5-ps and 4.7-ps durations were achieved at the output powers of 1.67 and 1.05 W, respectively, with the repetition rate being 97.09 MHz. Due to the flexible frequency-doubling characteristics of the optical superlattice, the mode-locking scheme based on intracavity SHG can easily extend ultrafast output from near-infrared to infrared so long as in the nonlinear crystal's transparent wavelength range.

This work was supported by the National Natural Science Foundation of China (61205140, 11021403, and 91321312), the Jiangsu Science Foundation (BK2011545), the State Key Program for Basic Research of China (2010CB630703 and 2011CBA00205), and PAPD of Jiangsu Higher Education Institutions.

References

1. R. Targ, B. C. Steakley, J. G. Hawley, L. L. Ames, P. Forney, D. Swanson, R. Stone, R. G. Otto, V. Zarifis, P. Brockman, R. S. Calloway, S. H. Klein, and P. Robinson, *Appl. Opt.* **35**, 7117 (1996).
2. P. A. Budni, L. A. Pomeranz, M. L. Lemons, C. A. Miller, J. R. Mosto, and E. P. Chicklis, *J. Opt. Soc. Am. B* **17**, 723 (2000).
3. H. Xiong, H. Xu, Y. X. Fu, J. P. Yao, B. Zeng, W. Chu, Y. Cheng, Z. Z. Xu, E. J. Takahashi, K. Midorikawa, X. Liu, and J. Chen, *Opt. Lett.* **34**, 1747 (2009).
4. T. Popmintchev, M. C. Chen, P. Arpin, M. M. Murnane, and H. C. Kapteyn, *Nat. Photonics* **4**, 822 (2010).
5. B. M. Walsh, *Laser Phys.* **19**, 855 (2009).
6. S. Amini-Nik, D. Kraemer, M. L. Cowan, K. Gunaratne, P. Nadesan, B. A. Alman, and R. J. D. Miller, *PLoS One* **5**, e13053 (2010).
7. J. F. Pinto, L. Esterowitz, and G. H. Rosenblatt, *Opt. Lett.* **17**, 731 (1992).
8. F. Heine, E. Heumann, G. Huber, and K. L. Schepler, *Appl. Phys. Lett.* **60**, 1161 (1992).
9. D. Gatti, G. Galzerano, A. Toncelli, M. Tonelli, and P. Laporta, *Appl. Phys. B* **86**, 269 (2007).
10. K. Yang, H. Bromberger, H. Ruf, H. Schäfer, J. Neuhaus, T. Dekorsy, C. V.-B. Grimm, M. Helm, K. Biermann, and H. Künzel, *Opt. Express* **18**, 6537 (2010).
11. A. Lagatsky, F. Fusari, S. Calvez, J. A. Gupta, V. E. Kisel, N. V. Kuleshov, C. T. A. Brown, M. D. Dawson, and W. Sibbett, *Opt. Lett.* **34**, 2587 (2009).
12. Q. Wang, J. Geng, T. Luo, and S. Jiang, *Opt. Lett.* **34**, 3616 (2009).
13. R. C. Sharp, D. E. Spock, N. Pan, and J. Elliot, *Opt. Lett.* **21**, 881 (1996).
14. S. Kivistö, T. Hakulinen, M. Guina, and O. G. Okhotnikov, *IEEE Photon. Technol. Lett.* **19**, 934 (2007).
15. M. S. Gaponenko, V. E. Kisel, N. V. Kuleshov, A. M. Malyarevich, K. V. Yumashev, and A. A. Onushchenko, *Laser Phys. Lett.* **7**, 286 (2010).
16. I. A. Denisov, N. A. Skoptsov, M. S. Gaponenko, A. M. Malyarevich, K. V. Yumashev, and A. A. Lipovskii, *Opt. Lett.* **34**, 3403 (2009).
17. W. B. Cho, A. S. J. H. Yim, S. Y. Choi, S. Lee, F. Rotermund, U. Griebner, G. Steinmeyer, V. Petrov, X. Mateos, Ma. C. Pujol, J. J. Carvajal, M. Aguiló, and F. Díaz, *Opt. Express* **17**, 11007 (2009).
18. M. A. Solodyankin, E. D. Obraztsova, A. S. Lobach, A. I. Chernov, A. V. Tausenev, V. I. Konov, and E. M. Dianov, *Opt. Lett.* **33**, 1336 (2008).
19. K. Kieu and F. W. Wise, *IEEE Photon. Technol. Lett.* **21**, 128 (2009).
20. J. Liu, Y. G. Wang, Z. S. Qu, L. H. Zheng, L. B. Su, and J. Xu, *Laser Phys. Lett.* **9**, 15 (2012).
21. J. Ma, G. Q. Xie, P. Lv, W. L. Gao, P. Yuan, L. J. Qian, H. H. Yu, H. J. Zhang, J. Y. Wang, and D. Y. Tang, *Opt. Lett.* **37**, 2085 (2012).
22. K. A. Stankov and J. Jethwa, *Opt. Commun.* **66**, 41 (1988).
23. S. Mukhopadhyay, S. Mondal, S. P. Singh, A. Date, K. Hussain, and P. K. Datta, *Opt. Express* **21**, 454 (2013).
24. H. Iliev, I. Buchvarov, S. Kurimura, and V. Petrov, *Opt. Lett.* **35**, 1016 (2010).
25. H. Iliev, D. Chuchumishev, I. Buchvarov, and V. Petrov, *Opt. Express* **18**, 5754 (2010).
26. S. J. Holmgren, V. Pasiskevicius, and F. Laurell, *Opt. Express* **13**, 5270 (2005).
27. Y. F. Chen, S. W. Tsai, and S. C. Wang, *Appl. Phys. B* **72**, 395 (2001).
28. Y. H. Liu, Z. D. Xie, S. D. Pan, X. J. Lv, Y. Yuan, X. P. Hu, J. Lu, L. N. Zhao, C. D. Chen, G. Zhao, and S. N. Zhu, *Opt. Lett.* **36**, 698 (2011).
29. H. Iliev, I. Buchvarov, S. Kurimura, and V. Petrov, *Opt. Express* **19**, 21754 (2011).
30. S. N. Zhu, Y. Y. Zhu, Z. Y. Zhang, H. Su, H. F. Wang, J. F. Hong, C. Z. Ge, and N. B. Ming, *J. Appl. Phys.* **77**, 5481 (1995).
31. D. H. Jundt, *Opt. Lett.* **22**, 1553 (1997).